Catalysis Today, 8 (1990) 37–55
Elsevier Science Publishers B.V., Amsterdam

THE MOLECULAR STRUCTURES AND REACTIVITY OF SUPPORTED NIOBIUM OXIDE CATALYSTS

Jih-Mirn JEHNG and Israel E. WACHS
Zettlemoyer Center for Surface Studies, Department of Chemical Engineering, Lehigh University, Bethlehem, PA 18015, U.S.A.

ABSTRACT

The molecular structure-reactivity relationships for supported niobium oxide catalysts were achieved by combining Raman spectroscopy structural studies with chemical probes that measured the acidity and reactivity of the surface niobium oxide sites. The Raman spectra of niobium oxide compounds are related to the specific niobium oxide molecular structures. The molecular structures of the surface niobium oxide phases present in supported niobium oxide catalysts under ambient conditions, where adsorbed moisture is present, are controlled by the surface pH of the system. Basic surfaces result in the formation of highly distorted NbO_6 groups and acidic surfaces result in the formation of slightly distorted NbO_6, NbO_7, and NbO_8 groups. Under in situ conditions the adsorbed moisture desorbs upon heating and the surface niobium oxide overlayer on oxide supports become dehydrated. The dehydration process further distorts the highly distorted NbO_6 octahedra due to removal of the coordinated water, but does not perturb the slightly distorted NbO_6 octahedra. The highly distorted NbO_6 octahedra possess Nb=O bonds and are associated with Lewis acid sites. The slightly distorted NbO_6 octahedra as well as NbO_7 and NbO_8 groups only possess Nb-O bonds and are associated with Brønsted acid sites. The Lewis acid surface sites are present on all the supported niobium oxide systems, but the Brønsted acid surface sites are limited to the Nb_2O_5/Al_2O_3 and Nb_2O_5/SiO_2 systems. The surface niobium oxide Lewis acid sites are significantly more active when coordinated to the Al_2O_3 and SiO_2 surfaces than to the TiO_2, ZrO_2, and MgO surfaces (surface oxide-support interaction). Furthermore, these surface niobium oxide sites on SiO_2 behaves as redox sites and the surface niobium oxide on Al_2O_3 are acid sites during partial oxidation reactions.

I. INTRODUCTION

Supported niobium oxide catalysts possess a surface niobium oxide overlayer on a high surface area oxide support. The surface niobium oxide phase is formed by the reaction of a suitable niobium precursor (i.e., oxalate [1], alkoxide[2], or chloride [3]) with the surface hydroxyls of the oxide support

[4]. The physical and chemical properties of the surface niobium oxide can be quite different than those found in bulk Nb_2O_5 phases, and can also dramatically influence the properties of the oxide supports [5]. For example, the surface niobium oxide phases impart thermal stability to oxide supports at elevated temperatures [6,7], form strong acid centers on oxide supports [6,8,9], and are active for numerous catalytic reactions in the petrochemical (i.e., olefin metathesis, dimerization, and isomerization), petroleum (i.e., cracking, isomerization, and alkylation), and pollution control (NO_x reduction from stationary emissions) industries [5]. The molecular structures of these surface niobium oxide phases, however, have not received much attention and only preliminary Raman [1,7] and EXAFS [10,11] characterization studies have been reported. Consequently, in the present paper the molecular structures of the surface niobium oxide phases on Al_2O_3, TiO_2, ZrO_2, MgO, and SiO_2 supports will be investigated under ambient as well as in situ conditions with Raman spectroscopy, and related to the reactivity of the supported niobium oxide catalysts.

II. EXPERIMENTAL

The supported niobium oxide on Al_2O_3, TiO_2, ZrO_2, and SiO_2 catalysts were prepared by the incipient-wetness impregnation method using niobium oxalate/oxalic acid aqueous solutions [1]. The water sensitive MgO support required the use of niobium ethoxide/propanol solutions under a nitrogen environment for the preparation of the Nb_2O_5/MgO catalysts. All samples were dried at 110-120°C and calcined at 450/500°C. Niobium oxalate was supplied by Niobium Products Company (Pittsburgh, PA) with the following chemical analysis: 20.5% Nb_2O_5, 790 ppm Fe, 680 ppm Si, and 0.1% insolubles. Niobium ethoxide (99.999% purity) was purchased from Johnson Matthey (Ward Hill, MA). The oxide supports employed in the present investigation are: MgO (Fluka, ~80 m^2/g), Al_2O_3 (Harshaw, ~180 m^2/g), TiO_2 (Degussa, ~50 m^2/g), ZrO_2 (Degussa, ~39 m^2/g), and SiO_2 (Cab-O-Sil, ~275 m^2/g). The BET surface areas of the oxide supports and the supported niobium oxide catalysts were obtained with a Quantsorb surface area analyzer (Quantachrome corporation, Model OS-9).

Raman spectra were obtained with a Spex triplemate spectrometer (Model 1877) coupled to an EG&G intensified

photodiode array detector, cooled thermoelectrically to -35 C, and interfaced with an EG&G OMA III Optical Multichannel Analyzer (Model 1463). The samples were excited by the 514.5 nm line of the Ar^+ laser with 10-100 mw of power. The overall spectral resolution of the spectra was determined to be about 2 cm^{-1}. An in situ quartz cell was designed in order to investigate the Raman changes upon dehydration of the supported niobium oxide catalysts above room temperature. The surface acidity of supported niobium oxide catalysts was measured with an Analect FX-6160 FTIR sepctrometer by pyridine adsorption. Catalysis studies of the supported niobium oxide catalysts were performed with the methanol oxidation reaction. The reactor consists of a digital flow rate controller (Brooks), a tube furnace (Lindberg), a condenser and methanol reservoir, and a gas chromatograph (HP 5840).

III. NIOBIUM OXIDE SOLUTION CHEMISTRY

The supported niobium oxide catalysts contain significant amounts of adsorbed moisture under ambient conditions which influence the molecular structures of the surface metal oxide phases [12,13]. The molecular structures of the surface niobium oxide phases under ambient conditions, as will be shown below, are directly related to the various aqueous niobium oxide species. Thus, a brief discussion of the niobium oxide solution chemistry is warranted.

Different types of niobium oxide ionic species ($NbO_2(OH)_4^{-3}$, $Nb_6O_{19}^{-8}$, $H_xNb_6O_{19}^{-(8-x)}$ (x=1, 2, or 3), and $Nb_{12}O_{36}^{-12}$) exist in aqueous solutions, and the solution pH as well as niobium oxide concentration determine the specific niobium oxide ionic species (see Table I). The $NbO_2(OH)_4^{-3}$ monomer only exists in very basic and dilute solutions. At high pH (~14.5), the hexaniobate ionic species, $Nb_6O_{19}^{-8}$, exists in aqueous solutions. In the pH range between 14.5-11.5, equilibria between $Nb_6O_{19}^{-8}$ and protonated hexaniobate ionic species, $H_xNb_6O_{19}^{-(8-x)}$ (x=1,2,3), exist in aqueous solution. In the pH range between 11.5-6.5, protonated hexaniobate ionic species, $H_xNb_6O_{19}^{-(8-x)}$ (x=1,2,3) start to hydrolyze to form polymeric $Nb_{12}O_{36}^{-12}$ species. At low pH ($\leqslant$6.5), the hexaniobate ionic species polymerizes to form $Nb_{12}O_{36}^{-12}$ species as well as a $Nb_2O_5.nH_2O$ precipitate.

All the aqueous niobium oxide ionic species possess highly

distorted NbO_6 structures which are reflected in the strong Raman bands in the 860-901 cm^{-1} region [14,15]. The $Nb_2O_5.nH_2O$ precipitate, after drying at 120°C for 2 hours, possesses Raman features very similar to amorphous Nb_2O_5 [16]. In amorphous Nb_2O_5 the slightly distorted NbO_6, NbO_7, and NbO_8 sites give rise to a strong and broad Raman band at ~650 cm^{-1}. In addition, $Nb_2O_5.nH_2O$ also possesses a small amount of highly distorted NbO_6 sites which give rise to a weak Raman band at ~900 cm^{-1}. Thus, niobium oxide aqueous species possess highly distorted NbO_6 groups in basic solution and form a precipitate containing slightly distorted NbO_6, NbO_7, and NbO_8 groups in an acidic solution.

IV. MOLECULAR STRUCTURES OF SURFACE NIOBIUM OXIDE PHASES UNDER AMBIENT CONDITIONS

Under ambient conditions surface metal oxide overlayers on oxide supports are hydrated due to the presence of adsorbed moisture, and the moisture influences the molecular structures of these surface metal oxide phases [12,13]. The Raman frequencies of the supported niobium oxide catalysts under ambient conditions (spectra taken at room temperature and samples exposed to air) are tabulated in Table II. Recent Raman characterization studies of supported vanadium oxide, molybdenum oxide, tungsten oxide, and chromium oxide catalysts under ambient conditions have revealed that the molecular structures of the hydrated surface metal oxide phases are directly related to the surface pH of the aqueous film which is determined by the combined pH of the oxide support and the metal oxide overlayer [18].

In aqueous environments the oxide support equilibrates at the pH which results in net zero surface charge (point zero surface charge or isoelectric point). The pH at the point zero surface charge of the metal oxide supports and niobium oxide are [18,19]: MgO, pH=12; Al_2O_3, pH=9; TiO_2, pH=5-6; ZrO_2, pH=4-7; SiO_2, pH=~2; Nb_2O_5, pH=~0.5. For supported metal oxide catalysts, the point zero surface charge of such composite materials is determined by the combined pH of the oxide support and the metal oxide overlayer. The influence of the metal oxide overlayer on the point zero surface charge of the composite system is directly related to the surface coverage of the surface metal oxide phases [20]. Thus, the addition of surface niobium oxide (pH ~0.5) to oxide supports ($2 \leq pH \leq 12$) will always decrease the pH of the point zero surface charge, and the extent of the

decrease will be proportional to the surface niobium oxide coverage.

At low surface niobium oxide coverages of the supported niobium oxide catalysts, the surface pH under ambient conditions is dominated by the properties of the oxide support. The basic pH values of the MgO, pH=12, and Al_2O_3, pH=9, supports suggest, from Table I, that hexaniobate species ($H_xNb_6O_{19}^{-(8-x)}$ where x= 1,2,3) should be present with corresponding Raman bands at ~880 cm^{-1}. Indeed, at low surface coverages for Nb_2O_5/MgO and Nb_2O_5/Al_2O_3 only strong Raman bands are present at ~880 and ~900 cm^{-1}, respectively (see Table II). The somewhat acidic pH values of the TiO_2, pH=5-6, and ZrO_2, pH=4-7, supports suggest that the hexaniobate species should not be present in high concentrations (see Table I) and that $Nb_2O_5.nH_2O$ type structures, containing slightly distorted NbO_6 as well as NbO_7 and NbO_8 groups, should be present at ~650 cm^{-1} for Nb_2O_5/TiO_2 and Nb_2O_5/ZrO_2 at low surface coverages. Unfortunately, the strong vibrations of the TiO_2 and ZrO_2 supports in this region do not allow direct confirmation of such niobium oxide species. However, the extremely weak Raman bands for Nb_2O_5/TiO_2 and Nb_2O_5/ZrO_2 at ~895 and ~875 cm^{-1}, respectively, is consistent with this conclusion. For the acidic SiO_2 support with a pH value of ~2, $Nb_2O_5.nH_2O$ type structures with a Raman band at ~650 cm^{-1} would be expected, but weak SiO_2 vibrations in this region also prevent the detection of such surface niobium oxide Raman bands at low niobium oxide loading.

At high surface niobium oxide coverages of the supported niobium oxide catalysts, the surface pH under ambient conditions is significantly influenced by the acidic niobium oxide overlayer. Under acidic aqueous conditions the $Nb_2O_5.nH_2O$ type structures (see Table I), containing slightly distorted NbO_6 as well as NbO_7 and NbO_8 groups, should be present and give rise to a Raman band at ~650 cm^{-1}. Indeed, such Raman bands are observed at high loading for Nb_2O_5/Al_2O_3 and Nb_2O_5/SiO_2 catalysts. The thermal stability of these niobium oxide structures, however, are very different on the SiO_2 and Al_2O_3 structures. For Nb_2O_5/SiO_2, further calcination at 700°C shifts the Raman band from ~680 to ~700 cm^{-1} which is characteristic of crystalline Nb_2O_5 (TT). For Nb_2O_5/Al_2O_3, further calcination at 700°C does not shift the Raman band at ~650 cm^{-1}. Thus, it appears that on SiO_2 the surface niobium oxide phase at high loading is present as a bulk Nb_2O_5

phase which weakly interacts with the silica substrate, and that on Al_2O_3 the supported niobium oxide phase at high loading is present as a two-dimensional overlayer anchored to the alumina support. This conclusion is also consistent with X-ray photoelectron spectroscopy surface measurements of these two systems that show a low Nb/Si ratio and a much higher Nb/Al ratio. The complete absence of Raman bands at ~650 cm^{-1} for Nb_2O_5/MgO at high loading reveals that the extremely basic MgO support is dominating the surface pH. The strong vibrations of the TiO_2 and ZrO_2 supports in the ~650 cm^{-1} region prevented the direct detection of this species at high loadings of Nb_2O_5/TiO_2 and Nb_2O_5/ZrO_2.

In summary, the available Raman data under ambient conditions on supported niobium oxide catalysts is consistent with prior studies that the surface pH determines the molecular structures of the surface metal oxide phases [17]. At low surface coverages on basic oxide supports (MgO and Al_2O_3), hexaniobate-like surface species ($H_xNb_6O_{19}^{-(8-x)}$ where x= 1,2,3) appear to be present. The hexaniobate type surface species contain highly distorted NbO_6 octahedra. At high surface coverages on the Al_2O_3 support, hydrated niobium oxide-type surface species ($Nb_2O_5.nH_2O$) are also present. The hydrated niobium oxide-type surface species contain slightly distorted NbO_6 octahedra as well as slightly distorted NbO_7 and NbO_8 structures. The hydrated niobium oxide-type surface species probably also predominate at low surface coverages on the acidic oxide supports (TiO_2, ZrO_2, and SiO_2), but can not be detected due to overlap with the strong vibrations from the oxide supports. In addition, bulk Nb_2O_5 Raman bands at ~680 cm^{-1} could be observed above 19% Nb_2O_5/Al_2O_3, 5% Nb_2O_5/ZrO_2, and 2% Nb_2O_5/SiO_2 indicating that monolayer coverage, titration of reactive surface hydroxyls, had been achieved. Bulk Nb_2O_5 was not formed on MgO, even at the equivalent of two monolayers loading which suggests incorporation of Nb^{+5} into the MgO support due to the strong acid-base interaction (additional evidence is provided below from in situ Raman studies). Bulk Nb_2O_5 could not be detected on TiO_2 because of the very strong TiO_2 vibrations.

V. STRUCTURAL CHEMISTRY AND RAMAN SPECTRA OF NIOBIUM OXIDES

The relationships between niobium oxide structures and their

corresponding Raman spectra were systematically studied for various bulk niobium oxide compounds (see Table III). The Raman frequencies strongly depend on the bond order of the niobium oxide structure and a higher niobium oxygen bond order, corresponding to a shorter distance, shifts the Raman frequency to higher wavenumbers [21]. Niobium oxide compounds generally possess an octahedrally-coordinated NbO_6 structure with different extents of distortion due to corner or edge-shared NbO_6 polyhedra. The Nb^{+5} cation is very large and has difficulty fitting into an oxygen-anion tetrahedron [22]. Only a few niobium oxide compounds (i.e., $YNbO_4$, $YbNbO_4$, $LaNbO_4$, and $SmNbO_4$) can possess a tetrahedrally-coordinated NbO_4 structure which is similar to the scheelite-like structure. Occasionally, NbO_7 and NbO_8 structures can also be found in niobium oxide phases [16].

For the regular tetrahedral NbO_4 structures, the major Raman frequency appears in the 790-830 cm^{-1} region. In the slightly distorted octahedral NbO_6 structures the major Raman frequencies appear in the 500-700 cm^{-1} region, and in the highly distorted octahedral NbO_6 structures the major Raman frequencies appear in the 850-1000 cm^{-1} region. The distortions in the niobium oxide compounds are caused by the tilting of two adjacent NbO_6 octahedra and the off-center displacement of the Nb atom. For the occasional heptaniobate and octaniobate structures, the Raman band positions are very similar to those in NbO_6 containing structures and depend on the extent of distortions. Thus, the Raman spectra of the niobium oxide compounds are related to the specific niobium oxide molecular structures.

VI. MOLECULAR STRUCTURES OF SURFACE NIOBIUM OXIDE PHASES UNDER 'N SITU CONDITIONS

Under in situ conditions the adsorbed moisture desorbs upon heating and the surface metal oxide overlayers on oxide supports become dehydrated [12,13]. The molecular structures of the surface metal oxide phases are generally altered upon dehydration because the surface pH can only exert its influence via an aqueous environment. Consequently, Raman shifts upon dehydration constitute direct proof of a surface metal oxide phase and the removal of coordinated water [12,13]. The Raman band positions of the supported niobium oxide catalysts under in situ conditions (spectra taken at 50°C in a closed cell after being heated to 500°C in flowing oxygen) are shown in Table IV. Upon dehydration,

the surface niobium oxide Raman bands above 800 cm^{-1} experience a shift and the surface niobium oxide Raman bands between 600-700 cm^{-1} are not perturbed. Thus, the Raman bands appearing above 800 cm^{-1} are associated with surface niobium oxide phases and Raman bands appearing between 600-700 cm^{-1} as associated with either bulk niobium oxide phases or surface phases that still possess coordinated moisture as hydroxyl groups.

Multiple surface niobium oxide species with Raman bands in the 800-1000 cm^{-1} region are present in the supported niobium oxide catalysts. A surface niobium oxide Raman band is observed at ~985 cm^{-1} on all the oxide supports and reveals that the same surface niobium oxide species is present for all the supported niobium oxide catalysts. A Raman band at ~985 cm^{-1} is generally observed for highly distorted NbO_6 octahedra, see Table III, and is also present at the interfaces of layered niobium oxide compounds [21,23]. The somewhat lower Raman band position of the 1% Nb_2O_5/ZrO_2 are attibuted to the presence of surface Cl and F impurities which were detected with XPS only in this particualr sample. A second Raman band is observed at ~935 cm^{-1} on the ZrO_2, TiO_2 as well as Al_2O_3 supports, and is also assigned to a highly distorted NbO_6 octahedra with a slightly longer Nb=O bond. An additional Raman band is present at ~890 cm^{-1} on the Al_2O_3 and MgO supports which reflects the presence of another highly distorted NbO_6 octahedra that possess a Nb=O bond length similar to that found in hexaniobate compounds (see Table I). On the MgO support, however, the ~890 cm^{-1} Raman band essentially does not shift during hydration/dehydration experiments. The absence of crystalline Nb_2O_5 formation for Nb_2O_5/MgO at very high niobium oxide loadings and the insensitivity of this band to the desorption of moisture suggests that this species originates from Nb^{+5} incorporated into the MgO support surface. The Nb_2O_5/MgO system possesses an additional Raman band at ~833 cm^{-1} which coincides with the Raman position of both distorted NbO_6 octahedra and regular NbO_4 tetrahedra. Consequently, the molecular structure associated with this band can not be determined solely from Raman spectroscopy.

Only one surface niobium oxide species with a Raman band in the 600-700 cm^{-1} region is observed, and this niobium oxide structure is only found for Nb_2O_5/Al_2O_3 catalysts above 1/2 monolayer surface coverage. The Raman band position for this

species , ~ 647 cm^{-1}, coincides with Raman bands of slightly distorted NbO_6 octahedra as well as slightly distorted NbO_7 and NbO_8 units (see Table III) which also give rise to Raman features in this region. The Raman band at ~647 cm^{-1} for Nb_2O_5/Al_2O_3 is not due to bulk Nb_2O_5 because it is stable to thermal treatments and does not convert to crystalline Nb_2O_5 at elevated temperatures. Thus, the insensitivity of this Raman band to surface dehydration of Nb_2O_5/Al_2O_3 during in situ experiments may possibly be due to niobium oxide clusters or layered structures as well as the presence of coordinated moisture as hydroxyl groups [21]. Surface niobium oxide species possessing Raman bands in the 600-700 cm^{-1} region may also be present for Nb_2O_5/TiO_2 and Nb_2O_5/ZrO_2 but can not be observed by Raman spectroscopy because of the strong vibrations of the oxide supports in this region. Additional surface acidity characterization studies, to be discussed below, suggest that such surface niobium oxide species are not present on TiO_2 and ZrO_2. A Raman band at ~680 cm^{-1} is also observed above 2% Nb_2O_5/SiO_2, but this is assigned to a bulk Nb_2O_5 phase because its band position is very close to TT-Nb_2O_5 (~690 cm^{-1}) and it readily crystallizes upon heating to elevated temperatures.

The various surface niobium oxide structures present in the supported niobium oxide catalysts appear to be related to the oxide support surface hydroxyl chemistry [24]. The surface niobium oxide phases are formed by reaction of the niobium oxide precursor with the surface hydroxyl groups of the oxide supports which are observable with infrared spectroscopy [4,25]. The SiO_2 surface possesses only one kind of surface hydroxyl group and only one surface niobium oxide species (Raman band at ~980 cm^{-1}) is present. The TiO_2 and ZrO_2 surfaces possess two kinds of surface hydroxyl groups and two surface niobium oxide species (Raman band at ~985 and ~930 cm^{-1}) are present. The Al_2O_3 surface possesses at least 4 different surface hydroxyl groups and four surface niobium oxide sepcies (Raman bands at ~985, ~930, ~890, and ~647 cm^{-1}) are present. The MgO surface possesses one kind of surface hydroxyl group, but three different niobium oxide species are observed (Raman bands at ~985, ~890, and ~830 cm^{-1}). The multiple niobium oxide species present in the Nb_2O_5/MgO system are due to the strong acid-base interaction between Nb_2O_5 and MgO which results in the incorporation of niobium oxide into the MgO support surface as well as surface niobium oxide species. The

low surface hydroxyl concentration of the SiO_2 support [24], relative to the other oxide supports, is responsible for the low surface concentration of surface niobium oxide species and the formation of bulk Nb_2O_5 at very low niobium oxide loading.

VII. SURFACE ACIDITY OF SUPPORTED NIOBIUM OXIDE CATALYSTS

The Lewis acid and Brønsted acid surface sites present in the supported niobium oxide catalysts were investigated by infrared spectroscopy of pyridine adsorption [25], and the results are presented in Figures 1 and 2. The MgO and SiO_2 supports do not possess Lewis acid surface sites, but the addition of niobium oxide moderately increases the surface concentration of Lewis acid sites. The TiO_2 and ZrO_2 supports contain an intermediate amount of Lewis acid surface sites and the addition of niobium oxide moderately decreases the surface concentration of Lewis acid sites. The Al_2O_3 support contains a high concentration of Lewis acid surface sites which is modulated by the niobium oxide loading. None of the oxide supports possess Brønsted acid sites, but the addition of niobium oxide generates a fair amount of Brønsted acid surface sites for the Nb_2O_5/Al_2O_3 and Nb_2O_5/SiO_2 systems and a very small concentration of Brønsted acid surface sites for Nb_2O_5/TiO_2, Nb_2O_5/ZrO_2, and Nb_2O_5/MgO at high niobium oxide loading.

Comparison of the surface acidity measurements, Figures 1 and 2, with the preceding in situ Raman studies, Table IV, provides insight into the origin of the Lewis acid and Brønsted acid surface sites for supported niobium oxide catalysts. The surface niobium oxide Raman bands at ~985, ~935, ~890, and ~830 cm^{-1} are observed at low loadings and correspond to the presence of Lewis acid surface sites. These surface niobium oxide species, with the possible exception of the species responsible for the ~830 cm^{-1} Raman band, consist of highly distorted NbO_6 octahedra that possess Nb=O bonds. Thus, these highly distorted surface niobium oxide octahedra serve as coordinatively unsaturated surface acid sites. For the Nb_2O_5/MgO system, the ~890 cm^{-1} Raman band is probably not a Lewis acid surface site since it appears to be incorporated into the MgO support surface and would not be expected to be exposed. The appearance of the ~647 cm^{-1} Raman band corresponds to the formation of Brønsted acid surface sites at high loading on the Al_2O_3 support. Thus, the

slightly distorted surface niobium oxide octahedra as well as NbO_7 and NbO_8 structures are associated with protons that form Brønsted acid surface sites. The exact location of these protons are not known from the IR and Raman characterization studies.

The Brønsted acidity for the Nb_2O_5/SiO_2 system corresponds to the region where bulk Nb_2O_5 is present, and the maximum with niobium oxide loading suggests that there is a critical Nb_2O_5 particle size that maximizes the concentration of Brønsted acid surface sites. Bulk Nb_2O_5 is well known to possess Brønsted acid sites [26]. The small amount of Brønsted acid surface sites for 10% Nb_2O_5/TiO_2 and 10% Nb_2O_5/ZrO_2 are also attributed to the presence of bulk Nb_2O_5 since monolayer coverage of surface niobium oxide was exceeded for these samples. Furthermore, the absence of Brønsted acid surface sites for Nb_2O_5/TiO_2 and Nb_2O_5/ZrO_2 strongly suggests that the slightly distorted surface niobium oxide species responsible for the ~650 cm^{-1} Raman band is probably not present in these systems (recall that this region was overshadowed by the strong vibrations of the TiO_2 and ZrO_2 supports). The origin of the small amount of Brønsted acid surface sites at 15% Nb_2O_5/MgO is not known since bulk Nb_2O_5 and the slightly distorted surface niobium oxide species at ~650 cm^{-1} are not present in this sample.

In summary, the highly distorted surface NbO_6 octahedra sites correspond to the Lewis acid sites and the slightly distorted surface NbO_6 sites as well as NbO_7 and NbO_8 sites are associated with the Brønsted acid sites of supported niobium oxide catalysts. In addition, bulk Nb_2O_5 phases present in these systems will also give rise to Brønsted acid surface sites.

VIII. REACTIVITY OF SUPPORTED NIOBIUM OXIDE CATALYSTS

The catalytic properties of the supported niobium oxide catalysts were probed with the methanol oxidation reaction because of its ability to discriminate between surface acid sites, formation of dimethyl ether (CH_3OCH_3), and surface redox sites, formation of formaldehyde (HCHO) and methyl formate ($HCOOCH_3$). The influence of the surface niobium oxide overlayer on the catalytic activity of methanol oxidation over the series of supported niobium oxide catalysts is presented in Table V. The surface niobium oxide overlayer had almost no influence on the reactivity of the TiO_2, ZrO_2, and MgO supports. In contrast,

the surface niobium oxide overlayer significantly enhanced the reactivity of the Al_2O_3 and SiO_2 supports. Comparison of the reactivity data with the earlier characterization studies reveals that the reactivity of the Lewis acid surface sites, consisting of highly distorted NbO_6 octahedra, is strongly influenced by the specific oxide support since essentially the same sites are present on all the supports. Thus, the highly distorted NbO_6 Lewis acid sites are significantly more reactive when coordinated to the Al_2O_3 and SiO_2 surfaces than the TiO_2, ZrO_2, and MgO surfaces (surface oxide-support interaction).

The reactivity of Brønsted acid surface sites, consisting of slightly distorted NbO_6 octahedra as well as NbO_7 and NbO_8 groups, appears to be greater than the reactivity of the Lewis acid surface sites for methanol oxidation over Nb_2O_5/Al_2O_3. This is demonstrated by the more than two-fold increase in reactivity upon increasing 5% Nb_2O_5/Al_2O_3, possessing only Lewis acid surface sites, to 12% Nb_2O_5/Al_2O_3, possessing both Lewis and Brønsted surface acid sites. The dramatic decrease in reactivity for 19% Nb_2O_5/Al_2O_3 is attributed to self-poisoning of the extremely reactive catalyst (i.e. carbon deposition). The Brønsted acid surface sites present in Nb_2O_5/SiO_2 are associated with the bulk Nb_2O_5 phase and are less active than such sites on the alumina surface. Thus, the reactivity of the Brønsted acid surface sites also appear to be markedly influenced by the specific oxide support, and the coordinated niobium oxide on the alumina surface enhances the reactivity of these sites.

The influence of the surface niobium oxide overlayer on the selectivity of the methanol oxidation reaction over the series of supported niobium oxide catalysts is presented in Table VI. The high selectivity towards CH_3OCH_3 of the surface niobium oxide monolayers on TiO_2, ZrO_2, and Al_2O_3 reveals that predominantly only acid sites, and essentially no redox sites, are present on these oxide support surfaces. In contrast, the surface niobium oxide overlayer on SiO_2, $< 2\%$ Nb_2O_5/SiO_2, behaves predominantly as a redox site and exhibits a high selectivity towards HCHO and $HCOOCH_3$. Thus, the same Lewis acid surface site, consisting of a highly distorted NbO_6 octahedra, can behave as either an acid site or redox site depending on the specific oxide support to which it is coordinated. The decrease in selectivity towards HCHO and $HCOOCH_3$ and the simultaneous increase in CH_3OCH_3 selectivity above

2% Nb_2O_5/SiO_2 are due to the Brønsted acid surface sites on the bulk Nb_2O_5 particles present at these loadings. The selectivity pattern of the Nb_2O_5/MgO system is more complex because of the reaction products from the Lewis acid surface sites as well as the exposed MgO surface sites.

IX. CONCLUSIONS

The Raman spectra of the niobium oxide compounds are related to the specific niobium oxide molecular structures. Slightly and highly distorted NbO_6 octahedra are the preferred coordinations and NbO_4 tetrahedra, NbO_7 heptaniobate, and NbO_8 octaniobate are less common or rare. The molecular structures of the surface niobium oxide phases present in supported niobium oxide catalysts under ambient conditions, where adsorbed moisture is present, are controlled by the surface pH of the system. Basic surfaces result in the formation of highly distorted NbO_6 groups and acidic surfaces result in the formation of slightly distorted NbO_6, NbO_7, and NbO_8 groups. Under in situ conditions the adsorbed moisture desorbs upon heating and the surface niobium oxide overlayer on oxide supports become dehydrated. The dehydration process further distorts the highly distorted NbO_6 octahedra due to removal of the coordinated water, but does not perturb the slightly distorted NbO_6 octahedra. The highly distorted NbO_6 octahedra possess Nb=O bonds and are associated with Lewis acid sites. The slightly distorted NbO_6 octahedra as well as NbO_7 and NbO_8 groups only possess Nb-O bonds and are associated with Brønsted acid sites. The Lewis acid surface sites are present on all the supported niobium oxide systems, but the Brønsted acid surface sites are limited to the Nb_2O_5/Al_2O_3 and Nb_2O_5/SiO_2 systems. The surface niobium oxide Lewis acid sites are significantly more active when coordinated to the Al_2O_3 and SiO_2 surfaces than to the TiO_2, ZrO_2, and MgO surfaces (surface oxide-support interaction). Furthermore, these surface niobium oxide sites on SiO_2 behaves as redox sites and the surface niobium oxide on Al_2O_3 are acid sites during partial oxidation reactions. Thus, the molecular structure-reactivity relationships for supported niobium oxide catalysts were achieved by combining Raman spectroscopy structural studies with chemical probes that measured the acidity and reactivity of the surface niobium oxide sites.

ACKNOWLEDGMENT

Financial support for this work by Niobium Products Company, Inc. is gratefully acknowledged. We wish to thank A. Turek and G. Datka for the infrared acidity measurements.

REFERENCES

1. J. M. Jehng and I. E. Wachs, ACS Petroleum Chemistry Division Preprints, 34(3), (1989) 546.

2. E. I. Ko, R. Bafrali, N. T. Nuhfer, and N. J. Wagner, J. Catal. 95, (1985) 260.

3. Y. Wada, M. Inaida, Y. Murakami, and A. Morikawa, Bull. Chem. Soc. Jpn. 61, (1988) 3839.

4. E. DeCanio, J. M. Jehng, and I. E. Wachs, to be published.

5. I. E. Wachs, Proc. Intern. Conf. on Niobium and Tantalum, (1989) 679.

6. L. L. Murrell and D. C. Grenoble, U.S. Patent 4,415,480 (1983); L. L. Murrell, D. C. Grenoble, and C. J. Kim, U. S. Patent 4,233,139 (1980).

7. I. E. Wachs, J. M. Jehng, and F. D. Hardcastle, Solid State Ionics 32/33, (1989) 904.

8. L. L. Murrell, D. C. Grenoble, C. J. Kim, and N. C. Dispenziere, J. Catal. 107, (1987) 463.

9. S. Okazaki and T. Okuyama, Bull. Chem. Soc. Jpn. 56, (1983) 2159.

10. K. Asakura and Y. Iwasawa, Chem. Lett., (1986) 511.

11. K. Asakura and Y. Iwasawa, Chem. Lett., (1988) 633.

12. S. S. Chan, I. E. Wachs, L. L. Murrell, L. Wang, and W. K. Hall, J. Phys. Chem. 88, (1984) 5831.

13. I. E. Wachs, F. D. Hardcastle, and S. S. Chan, Spectroscopy 1, (1986) 30.

14. A. Goiffon and B. Spinner, Bull. Soc. Chimi. France 11/12, (1975) 2435.

15. A. Goiffon, R. Granger, C. Bockel, and B. Spinner, Rev. Chim. Minerale 10, (1973) 487.

16. L. A. Aleshina, V. P. Malnenko, A. D. Phouphanov, and N. M. Jakovleva, J. of Non-Cryst. Solids 87, (1986) 350-360.

17. G. Deo and I. E. Wachs, sumitted to J. Phys. Chem..

18. G. A. Park, Chem. Rev. 65, (1965) 177; Adv. Chem. Series 61, (1967) 121.

19. Y. S. Yin, A. Ougour, A. Auroux, and J. C. Vederine, Stud. in Surf. Sci. Catal. 48, (1989) 525.

20. F. J. Gil-Llamblas, A. M. Escudey, J. C. G. Fierro, and A. C. Agudo, J. Catal. 95, (1985) 520.

21. J. M. Jehng, Ph.D. Dissertation, Lehigh University (1990).

22. G. Blasse, J. Solid State Chem. 7, (1973) 169.

23. A. J. Jacobson, J. T. Lewandowski, and J. W. Johnson, J. of Less-Common Metals 116, (1986) 137.

24. H. P. Boehm and H. Knozinger in Catalysis-Science and Technology; J. R. Anderson and M. Boudart, Eds.; Springer-Verlag, West Berlin, Vol. 4 , (1983) 38.

25. J. Datka, A. Turek, J. M. Jehng, and I. E. Wachs, submitted to J. Catal..

26. K. Tanabe, Mat. Chem. and Phys. 17, (1987) 217.

TABLE I

The aqueous potassium niobate species and Raman bands relationships at a pH range from 14.5 to 0.55

Solution pH	Species	Raman bands (cm^{-1})
>14.5 (dilute)	$NbO_2(OH)_4^{-3}$	860(s), 825(w), 510(m), 350(m)
14.5	$Nb_6O_{19}^{-8}$	865(s), 815(w), 730 (w), 520(m), 290(s), 230(w)
11.5	$H_xNb_6O_{19}^{-(8-x)}$ (x=1,2,3)	880(s), 820(w), 520(m), 420(w), 290(w)
6.5	$Nb_{12}O_{36}^{-12}$ $Nb_2O_5 \cdot nH_2O$	901(s), 480(m), 420(w) 880(vw), 630(w)
3.65	$Nb_{12}O_{36}^{-12}$ $Nb_2O_5 \cdot nH_2O$	901(w), 420(w) 880(w), 630(m), 280(w)
0.55	$Nb_2O_5 \cdot nH_2O$	880(w), 630(s), 420(w), 280(w)

TABLE II

Raman bands of supported niobium oxide catalysts under ambient conditions (hydrated state)

Catalyst	BET Surface Area (m^2/g)	Raman Bands (cm^{-1})
5% Nb_2O_5/MgO	86	880(m), 450(w), 380(w), 230(w)
10% Nb_2O_5/MgO	75	880(s), 450(w), 380(w), 230(m)
5% Nb_2O_5/Al_2O_3	180	900(s), 230(m)
19% Nb_2O_5/Al_2O_3	151	890(s), 650(s), 230(s)
1% Nb_2O_5/TiO_2	48	895(w)
7% Nb_2O_5/TiO_2	45	930(w)
1% Nb_2O_5/ZrO_2	39	875(w)
5% Nb_2O_5/ZrO_2	40	890(w)
2% Nb_2O_5/SiO_2	265	not observed due to overlap with oxide support
4% Nb_2O_5/SiO_2	262	680(m), 230(m)

TABLE III

The relationships between niobium oxide structures and Raman frequencies

Symmetry	Raman Bands	Compounds
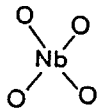	790-830 cm^{-1}	$YNbO_4$ $YbNbO_4$
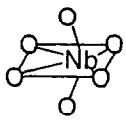 (NbO_7 and NbO_8)	500-700 cm^{-1}	Nb_2O_5 (amorphous, TT, T, and H) $LiNbO_3$ $NaNbO_3$ $KNbO_3$
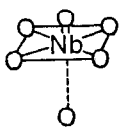	850-1000 cm^{-1}	Nb_2O_5 (H) $AlNbO_4$ $K_8Nb_6O_{19}$ $Nb(HC_2O_4)_5$

TABLE IV

Raman bands of supported niobium oxide catalysts under in situ conditions (dehydrated state)

Catalyst	Raman Bands (cm^{-1})
5%Nb_2O_5/MgO	986(w), 892(m), 833(s)
10%Nb_2O_5/MgO	985(m), 898(s), 834(s)
5%Nb_2O_5/Al_2O_3	980(s), 883(m)
19%Nb_2O_5/Al_2O_3	988(m), 938(s), 883(w), 647(s)
1%Nb_2O_5/TiO_2	983(m)
7%Nb_2O_5/TiO_2	985(s), 930(m)
1%Nb_2O_5/ZrO_2	956(s), 823(s)
5%Nb_2O_5/ZrO_2	988(s), 930(m)
2%Nb_2O_5/SiO_2	980(s)
4%Nb_2O_5/SiO_2	980(s), 680(m)

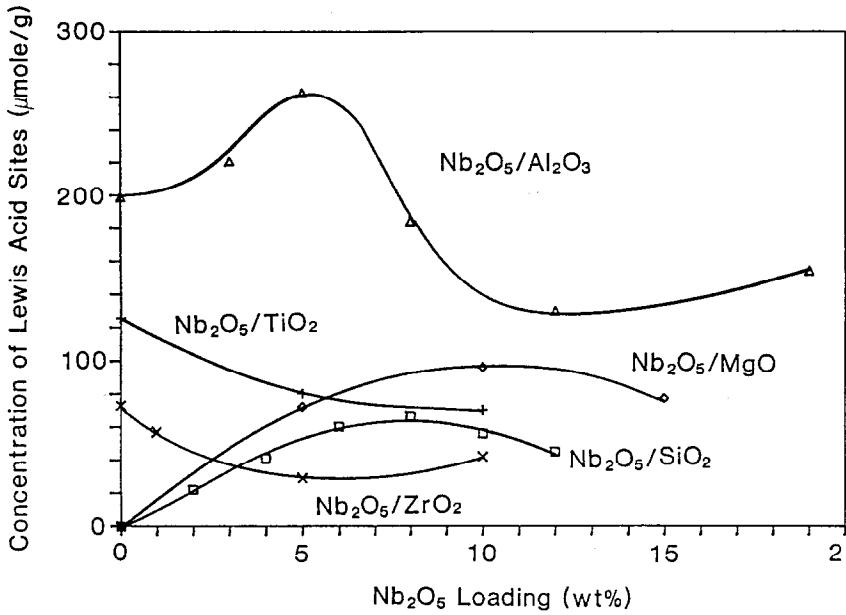

Fig 1: The Lewis acid surface sites present in the supported niobium oxide catalysts

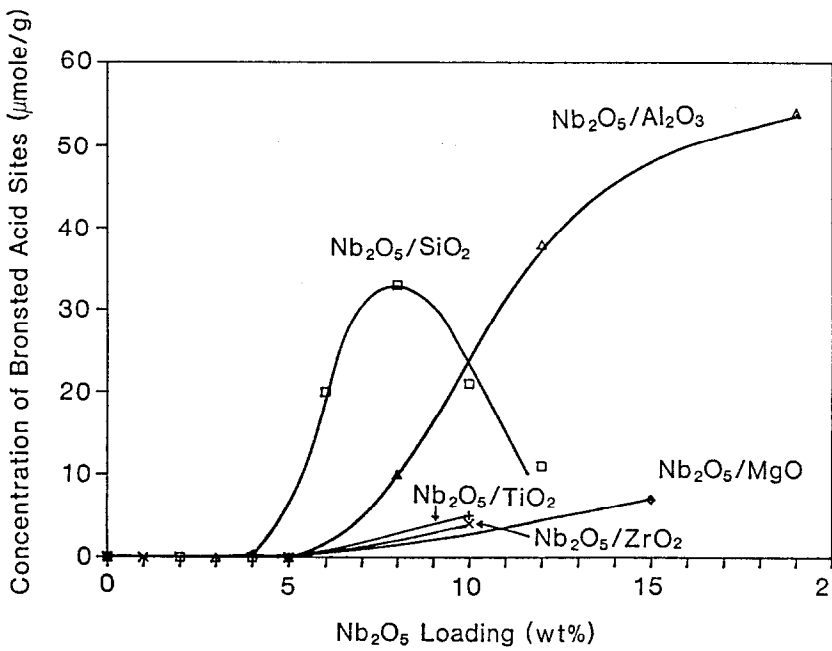

Fig. 2: The Bronsted acid surface sites present in the supported niobium oxide catalysts

TABLE V
The reactivity of methanol oxidation reaction over supported niobium oxide catalysts

Nb_2O_5 Loading (wt%)	Initial Rate [mmole/(g)(h)]				
	MgO	Al_2O_3	TiO_2	ZrO_2	SiO_2
0	8.4	64	2.1	7.3	0.7
0.2					21.4
1.0	2.8	323	2.5	7.1	26.5
2.0					38.4
2.5					26.2
3.0	6.8		3.9	5.3	
4.0					24.9
5.0	3.9	240	5.8	6.3	
6.0					15.4
7.0			6.2		
8.0		320			
10.0	2.0				
12.0		600			
19.0		75			

TABLE VI
The selectivity of methanol oxidation reaction over supported niobium oxide catalysts

Nb_2O_5 Loading (wt %)	MgO		Al_2O_3	TiO_2		ZrO_2		SiO_2	
	Redox	Acid	Acid	Redox	Acid	Redox	Acid	Redox	Acid
0	32.8	-	100	9.5	90.5	58.4	5.2	-	-
0.2								91.5	1.1
1	50.3	0.5	100	10.5	89.5	31.2	50.7	86.6	7.3
2								87.2	5.2
2.5								79.6	17.6
3	61.5	0.5	100	8.6	91.4	-	96.0	66.9	28.5
4									
5	71.4	2.1	100	3.7	96.3	-	98.0		
6								52.8	45.4
7				2.5	96.5	-			
10	56.5	27.9	100	1.4	97.2				

Rodox: HCHO and $HCOOCH_3$ Acid: CH_3OCH_3
CO/CO_2: 100-(Redox+Acid)